THE JOURNAL OF PHYSICAL CHEMISTRY B

Article

pubs.acs.org/JPCB

# Preferential Interactions between Lithium Chloride and Glucan Chains in *N,N*-Dimethylacetamide Drive Cellulose Dissolution

Adam S. Gross, Alexis T. Bell, and Jhih-Wei Chu*

Department of Chemical and Biomolecular Engineering, University of California, Berkeley, Berkeley, California 94720, United States

Supporting Information

**ABSTRACT:** Naturally occurring cellulose is crystalline as a consequence of the strong interactions between the glucan chains that comprise it and therefore is insoluble in most solvents. One of the few solvent systems able to dissolve cellulose is lithium chloride (LiCl) dissolved in *N,N*-dimethylacetamide (DMA). By an integrated application of all-atom molecular dynamics (MD) simulations, reaction path optimization, free-energy calculations, and a force-matching analysis of coarse-grained atomistic simulations, we establish that DMA-mediated preferential interactions of $Li^+$ cations and $Cl^-$ anions with glucan chains enable cellulose dissolution in LiCl/DMA. The relatively weak solvation of $Li^+$, $Cl^-$, and glucan chains by DMA results in strong effective interactions of $Li^+$ and $Cl^-$ ions with the glucans, leading to cellulose dissolution. The small size of the $Li^+$ cations allows them to strongly couple to multiple interaction sites on the glucan chains of cellulose, including the spatially restricted regions around the ether linkages connecting neighboring glucose residues. $Li^+$ cations were thus identified as the main component responsible for driving cellulose dissolution. The mechanism for explaining the solubility of cellulose in the LiCl/DMA system deduced from the analysis of atomistic-scale simulations conducted in this work is also consistent with most of the empirical observations related to cellulose dissolution in salt/amide solvent systems.

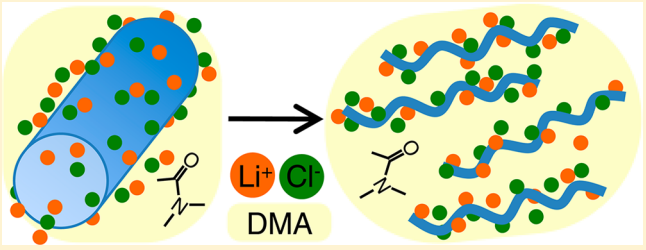


## INTRODUCTION

Lignocellulosic biomass is an attractive feedstock for the production of renewable fuels and chemicals because of the vast amounts of it available for use.[1,2] Cellulose, its most abundant component, is an aggregate of linear glucan polymers arranged into long, slender fibers called microfibrils located in the plant cell wall.[3,4] Native microfibrils are stabilized by a crystalline interaction network consisting of intrachain and interchain OH−O hydrogen bonds (HBs), as well as unconventional CH−O HBs and van der Waals (vdW) contacts between glucan chains of different sheets (intersheet interactions).[5,6] This network renders cellulose insoluble in most solvents.[7−11]

Despite its intrinsic stability, a handful of solvent systems have been found that can dissolve cellulose. Examples include ionic liquids (ILs), mixtures of *N*-methyl-*N*-morpholine-*N*-oxide (NMMO) and water, and aqueous transition metal complexes.[12,13] Another well-known cellulose solvent system is lithium chloride (LiCl) in *N,N*-dimethylacetamide (DMA) or its cyclic form, 1-methyl-2-pyrrolidinone (NMP).[14,15] This nonderivatizing solvent[16] has been shown to dissolve cellulose up to 10−15 wt %, with solubility proportional to LiCl concentration (1−10 wt %).[14,17] Cellulose can also be dissolved in other salt/amide solvent systems, but the solubility of cellulose tends to be significantly lower than that in LiCl/DMA.[18−22] Elucidation of how molecular coupling in these solvent systems disrupts the robust interaction network of cellulose can reveal the mechanisms of dissolution, and the resulting knowledge can contribute to the development of pretreatment technologies for biomass conversion.

Studies of the LiCl/DMA solvent system have provided information on the interactions of the dissolved salt with the amide. $Li^+$ cations have been shown to strongly associate with the carbonyl oxygen of DMA by $^{13}C$ NMR,[16] infrared spectroscopy,[23] X-ray crystallography,[24] and thermochemistry.[23−25] Quantum mechanical (QM) calculations of LiCl−DMA clusters also reveal strong DMA−$Li^+$ interactions.[26] For $Cl^-$ anions, experimental evidence does not indicate strong coupling to DMA. QM calculations suggest that the anions primarily interact with the methyl hydrogens of DMA.[26]

After cellulose is dissolved in LiCl/DMA, $Cl^-$ anions have been observed to replace the OH−O HBs between glucan chains with OH−$Cl^-$ HBs.[14,19] This role of $Cl^-$ in disrupting chain−chain interactions is similar to that of IL anions in cellulose-dissolving ILs.[27−31] $^7Li$ NMR spectra show that the chemical shift of cations in DMA is independent of LiCl concentration over a wide range, most likely because the DMA−$Li^+$ complex persists in these solutions. Conversely, the $^7Li$ NMR chemical shift has been observed to be a strong function of cellulose concentration, indicating close interactions between the cations and the sugars.[32] These observations indicate that both the DMA−$Li^+$ complex and the $Cl^-$ anions

**Received:** November 29, 2012
**Revised:** February 25, 2013
**Published:** February 26, 2013

   dx.doi.org/10.1021/jp311770u | *J. Phys. Chem. B* 2013, 117, 3280−3286

appear to favor coupling to cellulose over DMA in the DMA/LiCl solvent system. The emergent picture of how LiCl dissolved in DMA facilitates cellulose dissolution is thus direct interactions of $Li^+$ and $Cl^-$ ions with the polymer.[19,20] However, the specific roles and relative strengths of $Li^+$ and $Cl^-$ in coupling to glucose residues have yet to be resolved. Since cellulose dissolution does not take place after the addition of LiCl to water or most other solvents, the effective interactions between salt and sugar are likely significantly enhanced by DMA relative to other solvents. This suggests that the enhanced salt−cellulose coupling, termed preferential interactions, is a result of the balance between the interactions of $Li^+$, $Cl^-$, and glucan chain glucose residues with DMA. The theory of preferential interactions is well developed to rationalize how excipients such as urea and polyols destabilize or stabilize protein folding, respectively,[33,34] but has not yet been established for cellulose dissolution in salt/amide solvent mixtures. Solvent-mediated ion−solute interactions may also explain the observed capability of the LiCl/DMA system at dissolving polyamides.[35]

In this work, we present a quantitative analysis of the interactions between LiCl and cellulose in DMA using several molecular simulation methods. All-atom molecular dynamics (MD) simulations and free energy calculations for processes related to cellulose dissolution were conducted in four solvent systems: pure DMA, LiCl/DMA, pure water, and LiCl/water. In addition to computing the distributions of ion densities around cellulose in different states of dissolution, the results of atomistic simulations are subject to a coarse-grain (CG) force-matching (FM) analysis to quantify the strengths of LiCl−glucose residue interactions in different solvents. These methods also allow other unanswered questions related to cellulose dissolution in LiCl/DMA, such as how the specific coupling between glucose and solvent moieties leads to disruption of the cellulose interaction network, to be addressed.

## METHODS

**1. Reaction-Path Optimization and Potential of Mean Force (PMF) Calculations.** The PMF of peeling off a single glucan chain from the surface of a 12-chain, 10 glucose residues per chain, partial microfibril (Figure 1A,B) was calculated in DMA, LiCl/DMA, water, and LiCl/water. The arrangement of glucan chains in the model system represents the top three layers of a typically sized cellulose microfibril.[36] In the initial state of the deconstruction pathway, the partial microfibril is intact in the crystalline $I_\alpha$ configuration.[37] In the final state, six glucose residues of the top left corner chain are peeled off the microfibril surface from the reducing end (Figure 1A,B). To replicate the rigidity of an intact, full microfibril, harmonic restraints with 5 kcal/mol/Å$^2$ force constants were placed on the crystalline positions of all heavy ring atoms of sugar residues in the bottommost layer. To effectively represent the long lengths of cellulose microfibrils,[4] additional restraints of the same strength were put on the terminal carbons (C1 or C4 depending on the end) of the glucan chains, except for the free end of the peeled chain. For isolated glucan chains, these end restraints do not introduce noticeable effects on the distribution of the torsion angles of the glycosidic linkages.[31] The setup of the deconstruction pathway follows the same protocols reported in earlier works,[38,39] and the final pathway contains 32 replicas. The atomistic structures of the optimized pathway were used as the initial configurations of cellulose in the PMF calculations.

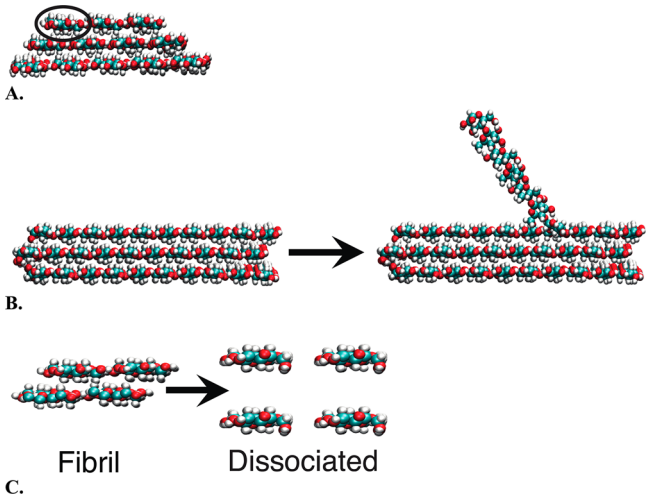


**Figure 1.** Molecular models and processes employed for investigating cellulose dissolution in this work. (A) Cross-section of the partial microfibril subject to deconstruction. The circled chain is detached from the microfibril surface in the deconstruction process. (B) Side view of the initial and final states of the partial microfibril in the deconstruction process. (C) Cross section of the fibril and dissociated states of the four chain system. The fibril state is in the crystalline $I_\alpha$ conformation. In the dissociated state, the chains are separated by ∼20 Å.

For the PMF calculations in each solvent system, the same number of solvent molecules is used to solvate all replicas. The DMA system contains 1750 solvent molecules. The LiCl/DMA system contains 1750 DMA molecules and 170 LiCl molecules, corresponding to a 4.5 wt % of salt, which is within the experimentally observed range of ion concentrations required to dissolve cellulose.[17] The LiCl/water system contains 8766 water molecules and 170 LiCl molecules, corresponding to the same molarity of salt as that in the LiCl/DMA system. The pure water system contains 6004 water molecules. All simulations were performed with the NAMD[40] software. Periodic boundary conditions were employed, and the system temperature and pressure were held constant at 350 K and 1 atm using a Langevin thermostat and Nose−Hoover Langevin barostat.[41,42] Cellulose, water, LiCl, and DMA were modeled using the CHARMM[43] carbohydrate force field,[44,45] TIP3P[46] force field, CHARMM ion force field,[47,48] and a newly developed force field created following the standardized CHARMM protocols for force field development (see the Supporting Information (SI)), respectively. For simulations involving the LiCl/DMA solvent system, ion−ion interactions were modified to better reproduce the experimentally measured thermodynamic behavior of LiCl in DMA (see the SI). The PMFs were calculated along the deconstruction pathway via integration of the mean force given by harmonic restraint potentials (force constant 5 kcal/mol/Å$^2$) placed on 32 equally spaced values of a collective variable.[38] The collective variable was the sum of two contact numbers. Because intersheet interactions are the main cause of cellulose insolubility, the first contact number was C−O contacts between the peeled chain and the two chains below it in the microfibril.[38] To prevent the off-path event of the peeled glucan chain collapsing back onto the far right side of the microfibril surface, C−O contacts between the peeled chain and the top right chain furthest from it in the top layer were also added to the collective variable. In conducting the PMF calculations in each solvent system, all 32


dx.doi.org/10.1021/jp311770u | J. Phys. Chem. B 2013, 117, 3280−3286

replicas were energy minimized, gradually heated to 350 K, and equilibrated for at least 5 ns before data collection in the production stage. The equilibration period ensures that the PMF profile has stabilized. Production runs of at least 15 ns were then used to calculate the PMFs of cellulose deconstruction.

**2. Simulation Models of Cellulose Dissolution.** As a complement to the free energy calculations of partial microfibril deconstruction described above, we performed MD simulations of four glucan chains, each 10 glucose residues long, solvated in both a fibril state and in a dissociated state (Figure 1C). The smaller system size allows for more extensive sampling and hence reduced statistical noise in the calculation of molecular structures and interaction forces. In the fibril state, the four chains are closely packed together in the crystalline cellulose $I_\alpha$ conformation,[37] while in the dissociated state they are separated by ~20 Å. Taken together, they represent the two end states of a dissolution process. To maintain the four-chain model in the fibril or dissociated state in the MD simulations, harmonic restraint potentials with a force constant of 5 kcal/mol/Å$^2$ were placed on the positions of the terminal carbons (C1 or C4) of each chain.[31] Both states were solvated by 1574 DMA molecules, 1574 DMA molecules and 152 LiCl molecules (4.5 wt % salt), or 8852 water molecules and 152 LiCl molecules. The molarity of salt is the same in the LiCl/DMA and LiCl/water systems. Other simulation protocols are the same as those described in the deconstruction section. During the equilibration stage, system volume, number of ions in contact with cellulose, and average cluster size of the ions were monitored until stable values were reached. Afterward, data from production runs of at least 30 ns were collected.

To compute the effective interactions between solvent, ion, and glucose moieties before and after dissolution, the coarse-graining scheme shown in Figure 2 is adopted. The $Li^+$ and $Cl^-$ ions are explicit CG sites in this analysis. The interaction potentials between CG sites were computed from the production-stage trajectories of the all-atom MD simulations using the force-matching (FM) method.[49] We also calculated the three-dimensional ion densities around DMA or the dissociated cellulose chains using a computational procedure described in previous work.[31] Other simulation and analysis details can be found in the SI.

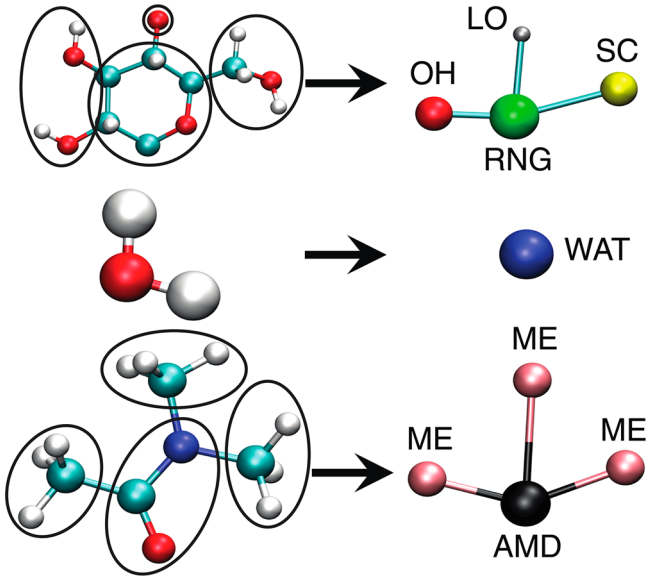


**Figure 2.** Coarse-graining scheme employed for glucose, water, and DMA used in computing the force-matched interaction potentials.

## RESULTS AND DISCUSSION

The calculated PMF profiles of cellulose deconstruction are shown in Figure 3. In LiCl/DMA, the free energy reduction of detaching a glucan chain from the microfibril surface is −1.3 ± 0.04 kcal/mol-glucose, demonstrating the cellulose dissolving capability of this solvent system. In pure DMA, pure water, and LiCl/water, monotonic increases in the PMF with progress of deconstruction indicate that these solvents cannot dissolve cellulose. In DMA the calculated free energy cost of peeling off the chain from the microfibril is 3.0 ± 0.11 kcal/mol-glucose, significantly higher than the value in water, 1.8 ± 0.03 kcal/mol-glucose. Also, the calculated free energy cost in LiCl/water, 1.6 ± 0.05 kcal/mol-glucose, is very close to that in pure water. Therefore, addition of LiCl does not qualitatively change the solubility behavior of cellulose in water but does do so in DMA.

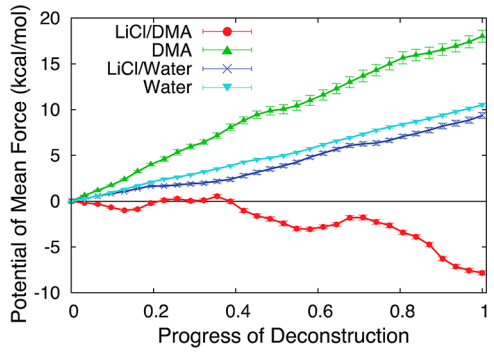


**Figure 3.** PMFs of cellulose deconstruction (Figure 1A,B) in LiCl/DMA, DMA, LiCl/water, and water.

Cellulose dissolution was also modeled by simulating a four-chain system in both a fibril and a dissociated state (Figure 1C). To inspect the emergent behaviors of preferential interactions, the average three-dimensional $Li^+$ and $Cl^-$ ion densities around the glucose residues of the dissociated chains were calculated. These densities, which are relative to the bulk value, are plotted from two orthogonal perspectives in Figure 4 for the LiCl/water system. For the dissociated state in water, ion localization around glucose residues relative to the bulk is not significant. Also, the high-density regions of the $Cl^-$ anions are closer to the glucose residues than those of the $Li^+$ cations. Local densities of $Cl^-$ are high near the equatorial OH groups of glucose, signifying OH−anion HBs. The high $Cl^-$ densities near the axial CH groups indicate the existence of CH−anion

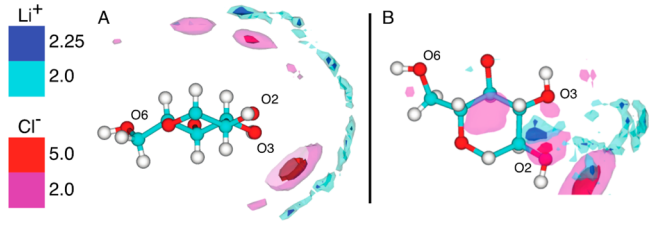


**Figure 4.** Average densities of $Li^+$ and $Cl^-$ ions around the dissociated glucan chains (Figure 1C) in water normalized by the bulk values. (A) Front view and (B) top view.


dx.doi.org/10.1021/jp311770u | J. Phys. Chem. B 2013, 117, 3280−3286

HBs as well. Although weaker than classical OH−acceptor interactions, CH−acceptor interactions possess the typical geometric and energetic characteristics of traditional HBs.[50−54] Overall however, cellulose−ion interactions in water are not sufficiently strong to cause cellulose dissolution (Figure 3)

The molar solubility of LiCl in DMA is an order of magnitude lower than that in water.[55,56] Similarly, the degree of ion−ion clustering in our simulations was a factor of 50% greater in DMA compared to that in water at equivalent molar LiCl concentrations (see SI Figures S2 and S3 for further information). The distribution of $Li^+$ and $Cl^-$ ions around DMA observed in all-atom MD simulations of the LiCl/DMA solvent system without cellulose also reveals clear molecular signatures of DMA being a poor solvent for the salt (details reported in the SI). In this solvent/dissolved-salt mixture, the CG interaction potentials calculated from the results of atomistic simulations indicate that ion−DMA interactions are highly frustrated, with the AMD−$Li^+$ and ME−$Cl^-$ interactions strongly attractive and the AMD−$Cl^-$ and ME−$Li^+$ interactions strongly repulsive. Besides being a poorer solvent for LiCl, DMA is also a poorer solvent than water for cellulose since the free energy cost of cellulose deconstruction in pure DMA is higher than that in pure water (Figure 3). Conversely, water is a poor solvent for cellulose but a good one for LiCl, and addition of LiCl to water does not change the inability of water to dissolve cellulose. Therefore, solvent properties appear to play an essential role in mediating the interactions between the added salt and cellulose to achieve dissolution.

In LiCl/DMA, the average three-dimensional $Li^+$ and $Cl^-$ ion density profiles normalized by bulk values around the dissociated glucan chains are shown in Figure 5A,B. The local

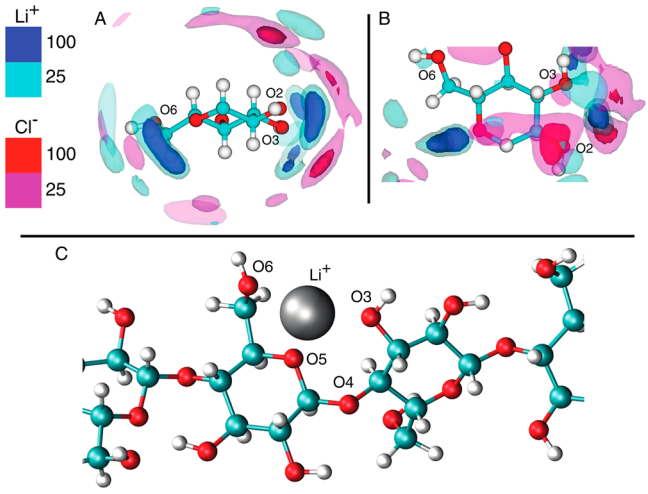


**Figure 5.** Average densities of $Li^+$ and $Cl^-$ ions around the dissociated glucan chains (Figure 1C) in DMA normalized by the bulk values. (A) Front view and (B) top view. (C) A configuration of $Li^+$ binding to the restricted region between neighboring glucose resides of a dissociated chain. This configuration is from a snapshot of the all-atom MD simulation.

enhancement of ion concentrations relative to the bulk is much greater in DMA than in water. $Li^+$ cations and $Cl^-$ anions bind tightly to sugar moieties from both the equatorial and axial directions of the sugar rings. The two ion types also strongly couple to each other near glucose residues to ensure local charge neutrality. In water, a good LiCl solvent, enhancement of ion concentration around the glucan chains is low, and strong anion−cation coupling is not observed around the polymer solute (Figure 4).

Ion localization in DMA is especially high near the oxygen-containing moieties of the glucan chains. Both $Li^+$ and $Cl^-$ densities are high by OH groups, and $Li^+$ density is also high near the O5 oxygen of the glucose ring. Also, in contrast to the ion distributions in water (Figure 4), in DMA the high-density regions of $Li^+$ are closer to the glucose residues than those of $Cl^-$. Therefore, cations appear to play a key role in driving cellulose dissolution in the LiCl/DMA system. OH−anion interactions have been identified as a molecular interaction that facilitates cellulose dissolution in LiCl/DMA,[19,20] but strong cellulose−$Li^+$ interactions have not been recognized. An interesting feature of the LiCl/DMA system is the accessibility by $Li^+$ cations to the interaction sites around a glucan chain that connect neighboring glucose residues. An example is shown in Figure 5C, wherein a single $Li^+$ interacts with the O6 and O5 oxygens of one glucose and the O4 and O3 oxygens of its neighbor. Also, in regards to the total number of sugar−ion contacts before and after dissolution, in DMA the average number of ions within 3 Å of a glucan chain is 8 (cation) and 16 (anion) greater in the dissociated state than in the fibril state (Figure 6). The corresponding increases are only 0.25 (cation)

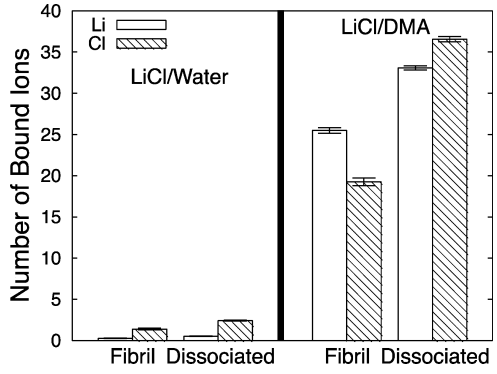


**Figure 6.** Average number of $Li^+$ and $Cl^-$ ions within 3 Å of cellulose atoms calculated from the MD simulations of the fibril and dissociated states of cellulose (Figure 1C) in LiCl/water and LiCl/DMA.

and 1 (anion) in water. This result shows that chain separation in the solvation environment created by DMA causes many more $Li^+$ and $Cl^-$ ions to associate with the glucan chains than in the environment created by water.

The observed preferential interactions in DMA of the $Li^+$ and $Cl^-$ ions with the glucose residues of the glucan chains that drive cellulose deconstruction can be revealed quantitatively by computation of the interaction potentials between CG moieties (Figure 2) using the force-matching method applied to the all-atom MD trajectories of the solvated fibril and dissociated states of cellulose shown in Figure 1C. The average interaction potentials of $Li^+$ and $Cl^-$ with the four CG sites of the glucose residues of both states are plotted in Figure 7A and 7B, respectively. The four glucan CG sites, SC, LO, RNG, and OH, are defined as the centers of mass of the atoms in the hydroxymethyl side group, the ether oxygen atom between neighboring glucose rings, the atoms within the glucose ring itself, and the oxygen and hydrogen atoms within OH groups directly off the glucose ring, respectively (see Figure 2). The rich features of these potentials are due to the complex liquid-state structures around the glucan chains. Nevertheless, the


dx.doi.org/10.1021/jp311770u | J. Phys. Chem. B 2013, 117, 3280−3286

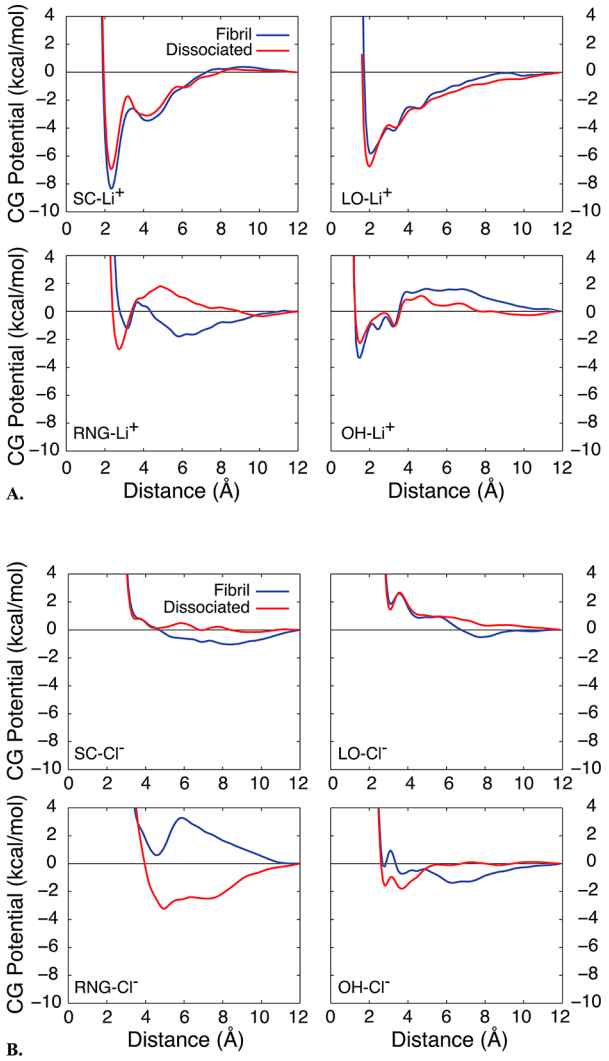


**Figure 7.** Interaction potentials of $Li^+$ and $Cl^-$ ions with the CG sites of the glucose residues of the glucan chains in LiCl/DMA. (A) $Li^+$ and (B) $Cl^-$. CG sites of glucose residues are shown in Figure 2.

occurrence of attractive interactions and well-defined first nearest-neighbor minima is clear.

For the $Li^+$ cation, SC−$Li^+$ and LO−$Li^+$ potentials in DMA are strongly attractive, with a strength greater than 6 kcal/mol at a short separation of ∼2 Å (Figure 7A). The profiles of the SC−$Li^+$ and LO−$Li^+$ potentials from the fibril and dissociated state simulations are similar, and so the greater number of ion−sugar contacts in the dissociated state (Figure 6) would promote cellulose dissolution. The attractive interactions between the OH site and $Li^+$ are also significant (>2 kcal/mol) in both the fibril and dissociated states. For the RNG−$Li^+$ potential, the minimum at ∼2.5 Å has a deeper well in the dissociated state than in the fibril state, indicating an intrinsic tendency for the cations to prefer interacting with cellulose in the dissolved state. Also, comparatively, cellulose−$Li^+$ interactions in water (Figure S15, SI) are much weaker than those in DMA.

Regarding $Cl^-$ anions, in DMA their interaction strengths with the CG sites of the glucose residues (Figure 7B) are significantly less than those of the $Li^+$ cations. $Cl^-$ anions only very weakly interact with the SC and LO sites, in contrast to the strong attractive SC−$Li^+$ and LO−$Li^+$ potentials. Also, the strengths of the glucan−$Cl^-$ interactions in DMA are similar to those in water (Figure S16, SI). For the RNG−$Cl^-$ and OH−$Cl^-$ potentials, the interactions are favorable in the dissociated state but repulsive in the fibril state. Therefore, anions do play a role in driving cellulose dissolution, but their contributions to this dissolution are less than those of the cations.

The results presented above indicate that direct interactions between $Li^+$ and glucose residues in DMA are indeed the main contributor to cellulose dissolution. $Cl^-$ anions do couple to the hydroxyl groups of glucose residues in DMA, but the solvent-mediated interactions between $Li^+$ and the glucose residues are much stronger. The small size of the $Li^+$ cations allows for multiple strong interaction sites with the glucan chains, especially around the linker oxygen moieties and hydroxymethyl side chain groups.

With regards to solvent−ion coupling, the calculated interaction potentials show that the amide group of DMA strongly interacts with $Li^+$, but this attractive interaction is counteracted by the highly repulsive ME−$Li^+$ interactions (Figure S9, SI). Therefore, $Li^+$ anions are highly frustrated in the bulk phase of DMA and hence favor coupling to glucan residues when cellulose is present. Similarly, $Cl^-$ anions interact attractively with the methyl groups of DMA but repulsively with the amide group, and so glucan−$Cl^-$ preferential interactions are also observed. However, $Cl^-$ anions cannot access as many interaction sites by the glucan chains as the $Li^+$ cations because of their larger size. Overall, glucose−$Cl^-$ interactions are weaker than glucose−$Li^+$ ones. Our calculations using all-atom models thus identify that the solvent-mediated preferential interactions of $Li^+$ cations with glucose residues of the glucan chains are the main contributor to cellulose dissolution in DMA. This theory is consistent with the empirical observation that NaCl or salts with larger cations dissolved in DMA are not able to dissolve cellulose,[14] but LiBr/DMA still can, although with a lower maximum solubility.[22]

## ■ CONCLUSIONS

Integrated application of all-atom MD simulations, reaction path optimization, free energy calculations, and a force-matching analysis of coarse-grained atomistic simulations has been used to develop a deeper understanding of the factors contributing to the dissolution of cellulose in LiCl/DMA. We find that solvent-mediated preferential interactions of $Li^+$ and $Cl^-$ ions with glucose residues enable cellulose dissolution. Detaching a glucan chain from a microfibril surface in LiCl/DMA is shown to lead to a free energy reduction. For the same process in pure DMA without the LiCl salt, a monotonic increase in the PMF with progress of deconstruction is observed. Analysis of three-dimensional density distributions and interaction potentials between CG sites indicates that DMA is a poor solvent for dissolving both LiCl and cellulose. As a result, in DMA, glucose residues and dissolved LiCl strongly couple to each other instead of to solvent molecules. In contrast, water is a good solvent for dissolving LiCl but a poor one for dissolving cellulose, and so solvent-mediated preferential interactions between LiCl and glucose residues do not occur in water. The small size of the $Li^+$ ions allows for many possible interaction sites with the glucose residues of the glucan chains, including the more restricted regions near the oxygen linkers that connect neighboring glucose residues. Consequently, the calculated strengths of the cellulose−$Li^+$ interactions are much stronger than those between cellulose and the larger $Cl^-$ anions.


dx.doi.org/10.1021/jp311770u | J. Phys. Chem. B 2013, 117, 3280−3286

A number of experimental observations are consistent with the aforementioned mechanism. First, the observed increase in cellulose solubility with LiCl concentration in DMA[17] can be attributed to higher concentrations of ions available to interact with the glucan chains and disrupt the intrinsic interaction network of cellulose. Second, substitution of DMA to other more polar substituted amides that better solvate LiCl, such as dimethylformamide, results in a weaker capability or total inability to dissolve cellulose.[14,18,21] On the basis of the mechanism discussed earlier, the key property of DMA in mediating strong LiCl–glucose residue coupling is its poor solvent capacity for both LiCl and cellulose. That is, although DMA only dissolves a limited amount of LiCl since it is a poor solvent for the salt, the combined effects of weak ion–solvent and cellulose–solvent coupling cause sufficiently strong preferential interactions between the salt and the glucose residues of the glucan chains to achieve cellulose dissolution. As discussed earlier, the small size of $Li^+$ is also important for binding to the spatially restricted interaction regions around the glucose residues. Therefore, we predict that replacing $Li^+$ with larger cations, e.g., sodium, potassium, calcium, and barium, results in a less effective cellulose solvent, as has been observed experimentally.[14] Conversely, replacing $Cl^-$ with $Br^-$ while keeping $Li^+$ as the cation leads to a weaker but still effective cellulose solvent.[22] Therefore, the importance of the $Cl^-$ anions to cellulose dissolution appears to be less than that of the $Li^+$ cations.[14,19,22] This experimental result is in agreement with our finding that anions do contribute to the disruption of the cellulose interaction network but have much weaker coupling strengths to the glucose residues than do the $Li^+$ cations. Consistent with this reasoning, we predict that at equivalent salt concentrations LiF/DMA should be a better cellulose solvent than LiCl/DMA, as $F^-$ is a smaller and stronger HB acceptor than $Cl^-$.[57]

Integration of the simulation results obtained in this work with the experimental observations of earlier studies indicates that the DMA-mediated preferential interactions between salt and sugar require a delicate balance of the interactions between the different components in the salt/cellulose/solvent system to give rise to the cellulose-dissolving capability. DMA being a poor solvent for both the salt and the substrate and a small cation size are identified as two key molecular features of this mechanism.

## ■ ASSOCIATED CONTENT

### Supporting Information

Modification of the LiCl ion–ion interaction potentials for simulation in DMA, validation of the DMA force field and force field parameters, discussion of LiCl solubility in DMA, and CG FM potentials between the glucose residues of the glucan chains and the remaining solvent groups not presented in the main text. This material is available free of charge via the Internet at http://pubs.acs.org.

## ■ AUTHOR INFORMATION

### Corresponding Author

*E-mail: jwchu@berkeley.edu. Phone: (510) 642-4398. Fax: (510) 642-4778.

### Notes

The authors declare no competing financial interest.

## ■ ACKNOWLEDGMENTS

This project was supported by the Energy Biosciences Institute (grant numbers OO7G03 and OO0J04). We also thank the computational resources provided by NERSC (National Energy Research Scientific Computing Center), which is supported by the Office of Science of the U.S. Department of Energy under Contract No. DE-AC02-05CH11231.

## ■ REFERENCES

(1) Huber, G. W.; Iborra, S.; Corma, A. Synthesis of Transportation Fuels from Biomass: Chemistry, Catalysts, and Engineering. *Chem. Rev.* **2006**, *106*, 4044–4098.

(2) Perlack, R. D. *Biomass as Feedstock for a Bioenergy and Bioproducts Industry: The Technical Feasability of a Billion-Ton Annual Supply*; Oak Ridge National Laboratory: Oak Ridge, TN, 2005.

(3) Ragauskas, A. J.; Williams, C. K.; Davison, B. H.; Britovsek, G.; Cairney, J.; Eckert, C. A.; Frederick, W. J.; Hallett, J. P.; Leak, D. J.; Liotta, C. L.; et al. The Path Forward for Biofuels and Biomaterials. *Science* **2006**, *311*, 484–489.

(4) Perez, S.; Mazeau, K. In *Polysaccharides: Structural Diversity and Functional Versatility*, 2nd ed.; Dumitriu, S., Ed.; Marcel Dekker: New York, 2005; pp 41–68.

(5) Himmel, M. E.; Ding, S. Y.; Johnson, D. K.; Adney, W. S.; Nimlos, M. R.; Brady, J. W.; Foust, T. D. Biomass Recalcitrance: Engineering Plants and Enzymes for Biofuels Production. *Science* **2007**, *315*, 804–807.

(6) Gross, A. S.; Chu, J.-W. On the Molecular Origins of Biomass Recalcitrance: The Interaction Network and Solvation Structures of Cellulose Microfibrils. *J. Phys. Chem. B* **2010**, *114*, 13333–13341.

(7) Wyman, C. E. What is (and Is Not) Vital to Advancing Cellulosic Ethanol. *Trends Biotechnol.* **2007**, *25*, 153–157.

(8) Yang, B.; Wyman, C. E. Pretreatment: The Key to Unlocking Low-Cost Cellulosic Ethanol. *Biofuels, Bioprod. Biorefin.* **2008**, *2*, 26–40.

(9) Wyman, C. E.; Dale, B. E.; Elander, R. T.; Holtzapple, M.; Ladisch, M. R.; Lee, Y. Y. Coordinated Development of Leading Biomass Pretreatment Technologies. *Bioresour. Technol.* **2005**, *96*, 1959–1966.

(10) Lynd, L. R.; Wyman, C. E.; Gerngross, T. U. Biocommodity Engineering. *Biotechnol. Prog.* **1999**, *15*, 777–793.

(11) Chang, R.; Gross, A. S.; Chu, J. W. Degree of Polymerization of Glucan Chains Shapes the Structure Fluctuations and Melting Thermodynamics of a Cellulose Microfibril. *J. Phys. Chem. B* **2012**, *116*, 8074–8083.

(12) Wertz, J. L.; Bedue, O.; Mercier, J. P. *Cellulose Science and Technology*; EPFL Press: Lausanne, 2010.

(13) Klemm, D. *Comprehensive Cellulose Chemistry*; Wiley-VCH, Weinheim: New York, 1998.

(14) Mccormick, C. L.; Callais, P. A.; Hutchinson, B. H. Solution Studies of Cellulose in Lithium-Chloride and N,N-Dimethylacetamide. *Macromolecules* **1985**, *18*, 2394–2401.

(15) Mccormick, C. L.; Lichatowich, D. K. Homogeneous Solution Reactions of Cellulose, Chitin, and Other Polysaccharides to Produce Controlled-Activity Pesticide Systems. *J. Polym. Sci., Polym. Lett.* **1979**, *17*, 479–484.

(16) El-Kafrawy, A. Investigation of the Cellulose LiCl Dimethylacetamide and Cellulose LiCl N-Methyl-2-Pyrrolidinone Solutions by C-13 NMR-Spectroscopy. *J. Appl. Polym. Sci.* **1982**, *27*, 2435–2443.

(17) Chrapava, S.; Touraud, D.; Rosenau, T.; Potthast, A.; Kunz, W. The Investigation of the Influence of Water and Temperature on the LiCl/DMAc/Cellulose System. *Phys. Chem. Chem. Phys.* **2003**, *5*, 1842–1847.

(18) Morgenstern, B.; Berger, W. Investigations About Dissolution of Cellulose in the LiCl/N,N-Dimethylformamide System. *Acta Polym.* **1993**, *44*, 100–102.

(19) Dawsey, T. R.; Mccormick, C. L. The Lithium Chloride/Dimethylacetamide Solvent for Cellulose - a Literature-Review. *J. Macromol. Sci., R. M. C.* **1990**, *C30*, 405–440.

(20) Morgenstern, B.; Kammer, H. W. Solvation in Cellulose-LiCl-DMAc Solutions. *Trends Polym. Sci.* **1996**, *4*, 87−92.
(21) Petrus, L.; Gray, D. G.; Bemiller, J. N. Homogeneous Alkylation of Cellulose in Lithium-Chloride Dimethyl-Sulfoxide Solvent with Dimsyl Sodium Activation - A Proposal for the Mechanism of Cellulose Dissolution in Licl/Me(2)So. *Carbohydr. Res.* **1995**, *268*, 319−323.
(22) Furuhata, K. I.; Koganei, K.; Chang, H. S.; Aoki, N.; Sakamoto, M. Dissolution of Cellulose in Lithium Bromide Organic-Solvent Systems and Homogeneous Bromination of Cellulose with N-Bromosuccinimide Triphenylphosphine in Lithium Bromide N,N-Dimethylacetamide. *Carbohydr. Res.* **1992**, *230*, 165−177.
(23) Balasubramanian, D.; Shaikh, R. Interaction of Lithium Salts with Model Amides. *Biopolymers* **1973**, *12*, 1639−1650.
(24) Bello, J.; Haas, D.; Bello, H. R. Interactions of Protein-Denaturing Salts with Model Amides. *Biochemistry* **1966**, *5*, 2539−2547.
(25) Nakamura, T. Complexing of Lithium Ion in Acetonitrile with Other Solvents - Investigation by Use of a Cation-Sensitive Glass-Electrode. *Bull. Chem. Soc. Jpn.* **1975**, *48*, 1447−1451.
(26) Zelenkovskii, V. M.; Fen'ko, L. A.; Bil'dyukevich, A. V. Quantum-Chemical Simulation of Interaction of Polycaproamide with a Lithium Chloride Solution in Dimethylacetamide. *Polym. Sci., Ser. B* **2006**, *48*, 28−31.
(27) Remsing, R. C.; Hernandez, G.; Swatloski, R. P.; Massefski, W. W.; Rogers, R. D.; Moyna, G. Solvation of Carbohydrates in N,N′-Dialkylimidazolium Ionic Liquids: A Multinuclear NMR Spectroscopy Study. *J. Phys. Chem. B* **2008**, *112*, 11071−11078.
(28) Remsing, R. C.; Swatloski, R. P.; Rogers, R. D.; Moyna, G. Mechanism of Cellulose Dissolution in the Ionic Liquid 1-N-Butyl-3-Methylimidazolium Chloride: A C-13 and Cl-35/37 NMR Relaxation Study on Model Systems. *Chem. Commun.* **2006**, 1271−1273.
(29) Youngs, T. G. A.; Holbrey, J. D.; Deetlefs, M.; Nieuwenhuyzen, M.; Gomes, M. F. C.; Hardacre, C. A Molecular Dynamics Study of Glucose Solvation in the Ionic Liquid 1,3-Dimethylimidazolium Chloride. *ChemPhysChem* **2006**, *7*, 2279−2281.
(30) Youngs, T. G. A.; Hardacre, C.; Holbrey, J. D. Glucose Solvation by the Ionic Liquid 1,3-Dimethylimidazolium Chloride: A Simulation Study. *J. Phys. Chem. B* **2007**, *111*, 13765−13774.
(31) Gross, A. S.; Bell, A. T.; Chu, J.-W. Thermodynamics of Cellulose Solvation in Water and the Ionic Liquid 1-Butyl-3-Methylimidazolim Chloride. *J. Phys. Chem. B* **2011**, *115*, 13433−13440.
(32) Morgenstern, B.; Kammer, H. W.; Berger, W.; Skrabal, P. Li-7-NMR Study on Cellulose LiCl N.N-Dimethylacetamide Solutions. *Acta Polym.* **1992**, *43*, 356−357.
(33) Hua, L.; Zhou, R. H.; Thirumalai, D.; Berne, B. J. Urea Denaturation by Stronger Dispersion Interactions with Proteins than Water Implies a 2-Stage Unfolding. *Proc. Natl. Acad. Sci. U.S.A.* **2008**, *105*, 16928−16933.
(34) Street, T. O.; Bolen, D. W.; Rose, G. D. A Molecular Mechanism for Osmolyte-Induced Protein Stability. *Proc. Natl. Acad. Sci. U.S.A.* **2006**, *103*, 13997−14002.
(35) Panar, M.; Beste, L. F. Structure of Poly(1,4-Benzamide) Solutions. *Macromolecules* **1977**, *10*, 1401−1406.
(36) Ding, S. Y.; Himmel, M. E. The Maize Primary Cell Wall Microfibril: A New Model Derived from Direct Visualization. *J. Agric. Food Chem.* **2006**, *54*, 597−606.
(37) Nishiyama, Y.; Sugiyama, J.; Chanzy, H.; Langan, P. Crystal Structure and Hydrogen Bonding System in Cellulose 1(alpha), from Synchrotron X-Ray and Neutron Fiber Diffraction. *J. Am. Chem. Soc.* **2003**, *125*, 14300−14306.
(38) Cho, H. M.; Gross, A. S.; Chu, J.-W. Dissecting Force Interactions in Cellulose Deconstruction Reveals the Required Solvent Versatility for Overcoming Biomass Recalcitrance. *J. Am. Chem. Soc.* **2011**, *133*, 14033−14041.
(39) Brokaw, J. B.; Haas, K. R.; Chu, J. W. Reaction Path Optimization with Holonomic Constraints and Kinetic Energy Potentials. *J. Chem. Theory Comput.* **2009**, *5*, 2050−2061.
(40) Phillips, J. C.; Braun, R.; Wang, W.; Gumbart, J.; Tajkhorshid, E.; Villa, E.; Chipot, C.; Skeel, R. D.; Kale, L.; Schulten, K. Scalable Molecular Dynamics with NAMD. *J. Comput. Chem.* **2005**, *26*, 1781−1802.
(41) Martyna, G. J.; Tobias, D. J.; Klein, M. L. Constant-Pressure Molecular-Dynamics Algorithms. *J. Chem. Phys.* **1994**, *101*, 4177−4189.
(42) Feller, S. E.; Zhang, Y. H.; Pastor, R. W.; Brooks, B. R. Constant-Pressure Molecular-Dynamics Simulation - the Langevin Piston Method. *J. Chem. Phys.* **1995**, *103*, 4613−4621.
(43) Brooks, B. R.; Bruccoleri, R. E.; Olafson, B. D.; States, D. J.; Swaminathan, S.; Karplus, M. Charmm - a Program for Macromolecular Energy, Minimization, and Dynamics Calculations. *J. Comput. Chem.* **1983**, *4*, 187−217.
(44) Guvench, O.; Greene, S. N.; Kamath, G.; Brady, J. W.; Venable, R. M.; Pastor, R. W.; Mackerell, A. D. Additive Empirical Force Field for Hexopyranose Monosaccharides. *J. Comput. Chem.* **2008**, *29*, 2543−2564.
(45) Guvench, O.; Hatcher, E.; Venable, R. M.; Pastor, R. W.; MacKerell, A. D. CHARMM Additive All-Atom Force Field for Glycosidic Linkages between Hexopyranoses. *J. Chem. Theory Comput.* **2009**, *5*, 2353−2370.
(46) Jorgensen, W. L.; Chandrasekhar, J.; Madura, J. D.; Impey, R. W.; Klein, M. L. Comparison of Simple Potential Functions for Simulating Liquid Water. *J. Chem. Phys.* **1983**, *79*, 926−935.
(47) Beglov, D.; Roux, B. Finite Representation of an Infinite Bulk System - Solvent Boundary Potential for Computer-Simulations. *J. Chem. Phys.* **1994**, *100*, 9050−9063.
(48) Lamoureux, G.; Roux, B. Absolute Hydration Free Energy Scale for Alkali and Halide Ions Established from Simulations with a Polarizable Force Field. *J. Phys. Chem. B* **2006**, *110*, 3308−3322.
(49) Noid, W. G.; Chu, J. W.; Ayton, G. S.; Voth, G. A. Multiscale Coarse-Graining and Structural Correlations: Connections to Liquid-State Theory. *J. Phys. Chem. B* **2007**, *111*, 4116−4127.
(50) Steiner, T.; Saenger, W. Geometry of C-H...O Hydrogen-Bonds in Carbohydrate Crystal-Structures - Analysis of Neutron-Diffraction Data. *J. Am. Chem. Soc.* **1992**, *114*, 10146−10154.
(51) Calhorda, M. J. Weak Hydrogen Bonds: Theoretical Studies. *Chem. Commun.* **2000**, 801−809.
(52) Koch, U.; Popelier, P. L. A. Characterization of C-H-O Hydrogen-Bonds on the Basis of the Charge-Density. *J. Phys. Chem.* **1995**, *99*, 9747−9754.
(53) Steiner, T. Unrolling the Hydrogen Bond Properties of C-H Center Dot Center Dot Center Dot O Interactions. *Chem. Commun.* **1997**, 727−734.
(54) Taylor, R.; Kennard, O. Crystallographic Evidence for the Existence of C-H...O, C-H...N, and C-H...C1 Hydrogen-Bonds. *J. Am. Chem. Soc.* **1982**, *104*, 5063−5070.
(55) Cohen-Adas, R.; Lorimer, J. W. *Solubility Data Series*; Pergamon Press: Elmsford, NY, 1991; Vol. *47*.
(56) Potthast, A.; Rosenau, T.; Buchner, R.; Roder, T.; Ebner, G.; Bruglachner, H.; Sixta, H.; Kosma, P. The cellulose SolventSsystem N,N-Dimethylacetamide/Lithium Chloride Revisited: The Effect of Water on Physicochemical Properties and Chemical Stability. *Cellulose* **2002**, *9*, 41−53.
(57) Kovacs, A.; Varga, Z. Halogen Acceptors in Hydrogen Bonding. *Coord. Chem. Rev.* **2006**, *250*, 710−727.